Published in final edited form as:
Dev Cell. 2006 January ; 10(1): 71–80. doi:10.1016/j.devcel.2005.12.003.

Crkl Deficiency Disrupts Fgf8 Signaling in a Mouse Model of *22q11* Deletion Syndromes

Anne M. Moon[1,*], **Deborah L. Guris**[2], **Ji-heui Seo**[2], **Leiming Li**[2], **Jennetta Hammond**[1], **Amy Talbot**[1], and **Akira Imamoto**[2,*]

1 *Departments of Pediatrics and Neurobiology and Anatomy and Program in Human Molecular Biology and Genetics University of Utah School of Medicine Salt Lake City, Utah 84112*

2 *The Ben May Institute for Cancer Research and Center for Molecular Oncology Committee on Developmental Biology The University of Chicago Chicago, Illinois 60637*

Summary

Deletions on chromosome 22q11.21 disrupt pharyngeal and cardiac development and cause DiGeorge and related human syndromes. *CRKL* (*CRK-Like*) lies within 22q11.21, and *Crkl*$^{-/-}$ mice have phenotypic features of 22q11 deletion (*del22q11*) syndromes. While human FGF8 does not localize to 22q11, deficiency of Fgf8 also generates many features of *del22q11* syndrome in mice. Since Fgf8 signals via receptor-type tyrosine kinases, and Crk family adaptor proteins transduce intracellular signals downstream of tyrosine kinases, we investigated whether Crkl mediates Fgf8 signaling. In addition to discovering genetic interactions between *Crkl* and *Fgf8* during morphogenesis of structures affected in *del22q11* syndrome, we found that Fgf8 induces tyrosine phosphorylation of FgfRs 1 and 2 and their binding to Crkl. Crkl is required for normal cellular responses to Fgf8, including survival and migration, Erk activation, and target gene expression. These findings provide mechanistic insight into disrupted intercellular interactions in the pathogenesis of malformations seen in *del22q11* syndrome.

Introduction

Patients with DiGeorge, velocardiofacial, and CATCH-22 syndromes suffer serious morbidity and mortality. These "*del22q11*" syndromes include characteristic malformations of the heart, outflow tract, and vasculature, in addition to craniofacial defects and immune dysfunction due to abnormal thymic development. Although a number of loci within *del22q11* contribute to these phenotypes, the functions of *del22q11* genes in specific molecular pathways mediating intercellular interactions during cardiovascular and pharyngeal development have yet to be determined (Lindsay, 2001; Scambler, 2000; Schinke and Izumo, 2001; Yamagishi and Srivastava, 2003).

CRKL (CRK-Like) is located within the typically deleted region in patients with *del22q11*, and disruption of its mouse ortholog, *Crkl*, causes cardiovascular, craniofacial, and glandular features of *del22q11* syndrome (Guris et al., 2001). *CRKL* and related family members encode adaptor proteins that play important roles during intercellular signaling; they function in recruitment and activation of signaling complexes at focal adhesions and transduce intracellular signals downstream of several classes of RTKs (Feller, 2001; Klint and Claesson-Welsh, 1999; Li et al., 2003).

*Correspondence: anne.moon@genetics.utah.edu(A.M.M.); aimamoto@uchicago.edu (A.I.)

Fgf8 encodes a secreted signaling protein required in multiple expression domains to support normal cardiovascular development (Macatee et al., 2003; E. Park and A.M.M., submitted). FGF8 is not located on human 22q11; however, Fgf8 deficiency during mouse embryogenesis produces a complex perinatal-lethal phenotype that phenocopies human *del22q11* syndrome (Abu-Issa et al., 2002; Frank et al., 2002). Although it is not yet known which Fgf receptors (FgfRs) specifically transduce Fgf8 signals in vivo during cardiovascular and pharyngeal development, shared gastrulation, limb, craniofacial, and vascular defects caused by mutations in Fgf8, FgfR1, and FgfR2 in mice suggest important roles for FgfRs 1 and 2 in these processes (Arman et al., 1998; Celli et al., 1998; Deng et al., 1994, 1997; Rossant et al., 1997; Sun et al., 1999; Trokovic et al., 2003; Xu et al., 1998; L. Francis and A.M.M., unpublished data).

Formation of the Fgf ligand/FgfR complex causes receptor autophosphorylation and triggers multiple intracellular signaling cascades. Activated FgfRs bind Src-homology2 (SH2) signaling proteins such as PLCγ and Shp-2 (Bottcher and Niehrs, 2005). A functional link between Fgf signaling and Crk activity during embryogenesis was suggested by the observation that transduction of FgfR1-mediated intracellular signals in endothelial cells depends on ligand-induced tyrosine phosphorylation of FgfR1 on a residue bound by Crk (Larsson et al., 1999).

These lines of evidence led us to hypothesize that FGF8 and the adaptor protein CRKL function in a common molecular pathway that, when disrupted by haploinsufficiency of CRKL, contributes to the pathogenesis of human *del22q11* syndrome. We tested this hypothesis by investigating the role of Crkl in Fgf8/FgfR signal transduction required for normal pharyngeal arch and cardiovascular development in genetically engineered mice and embryonic cells derived therefrom.

Results

Fgf8 and *Crkl* Genetically Interact during Mouse Morphogenesis

We used an Fgf8;Crkl allelic series in genetically engineered mice to determine if Crkl and Fgf8 cooperatively affect embryonic survival and morphogenesis of Fgf8-sensitive structures including the cardiovascular system, pharyngeal glands, and the craniofacial and appendicular skeleton.

The fourth pharyngeal arch artery (PAA4) ultimately forms the arch of the aorta; disrupted formation or remodeling of PAA4 results in interrupted aortic arch or right aortic arch as well as subclavian artery anomalies (vascular defects seen in human *del22q11* syndrome). PAA4 formation occurs normally in Fgf8 null heterozygotes ($Fgf8^{+/-}$), but it is disrupted at lower levels of Fgf8 that occur in Fgf8 hypomorphic and conditional mutants, revealing the extreme sensitivity of PAA4 vasculogenesis to Fgf8 levels in the developing pharynx (Abu-Issa et al., 2002; Frank et al., 2002; Macatee et al., 2003). Although PAA4 forms normally in $Crkl^{-/-}$ embryos, combined Crkl/Fgf8 deficiency profoundly disrupts PAA4 formation: 50% of $Fgf8^{+/-}$;$Crkl^{+/-}$ and 90% of $Fgf8^{+/-}$;$Crkl^{-/-}$ mutants have aplastic or hypoplastic fourth PAAs at embryonic day (E) 10.5 ($p = 0.05$ and $p < 0.0001$, respectively, relative to $Crkl^{-/-}$; Figures 1A-1D). Some $Fgf8^{+/-}$;$Crkl^{+/-}$ and $Fgf8^{+/-}$;$Crkl^{-/-}$ mutants die at mid-gestation and display aortic sac dilatation and no caudal PAAs (12% and 14%, respectively,Figure 1D); this phenotype was not observed in $Crkl^{-/-}$ embryos. Recovery from PAA4 formation defects observed at E10.5 can occur during remodeling; however, decreased Fgf8;Crkl dosage frequently prevents recovery, resulting in aortic interruptions and subclavian artery defects in E15.5 $Fgf8^{+/-}$;$Crkl^{-/-}$ mutants (Figure 1F;Table 1).

Ablation of a single copy of Fgf8 in Crkl null homozygotes increases the incidence and severity of intracardiac and outflow tract defects (Table 1; Figure 1). Atrioventricular valve dysplasias,

which reflect abnormal formation and/or remodeling of the outflow and endocardial cushions, are more common and markedly more severe in $Fgf8^{+/-};Crkl^{-/-}$ mutants compared to $Crkl^{-/-}$ (Figures 1H-1L). Survival of $Fgf8^{+/-};Crkl^{+/-}$ and $Fgf8^{+/-};Crkl^{-/-}$ mutants to E15.5 is also compromised relative to single heterozygotes and $Crkl^{-/-}$ mutants (data not shown). Thus, Crkl deficiency reduces the effective Fgf8 signals required to support early cardiovascular development and embryonic survival.

The pharyngeal pouch endoderm gives rise to the primordia of the thymus and parathyroids; defects in these tissues contribute to the morbidity of DiGeorge syndrome patients in the form of immunodeficiency and hypocalcemia, respectively. Fgf8 hypomorphs have frequent aplasia of these glands and associated T cell deficiency (Frank et al., 2002). The size and location of the thymus and parathyroids are normal in Fgf8 or Crkl heterozygotes; however, $Fgf8^{+/-};Crkl^{+/-}$ mutants have the same incidence of glandular ectopy as $Crkl^{-/-}$ embryos. Moreover, glandular phenotypes are exacerbated in $Fgf8^{+/-};Crkl^{-/-}$ mutants (Figure 1F; Table 1), indicating a dosage-sensitive interaction between Fgf8 and Crkl during pharyngeal pouch development.

Humans with *del22q11* have variable appendicular and craniofacial skeletal malformations and short stature (Bird and Scambler, 2000; Emanuel et al., 2001; Motzkin et al., 1993). Patterning, outgrowth, and the ultimate length of limb bony elements are all sensitive to Fgf8 signaling from epithelial cells to underlying mesenchyme (Boulet et al., 2004; Lewandoski et al., 2000; Moon and Capecchi, 2000). Femurs of $Fgf8^{+/-};Crkl^{+/-}$ and $Fgf8^{+/-};Crkl^{-/-}$ mutants are an average of 35% shorter than $Fgf8^{+/-}$ and $Crkl^{-/-}$ littermates (Figures 1O-1Q). Cleft palate and mandibular hypoplasia are frequently observed in patients with *del22q11* syndrome, and in Fgf8 hypomorphic or conditional mutant mice (Abu-Issa et al., 2002; Frank et al., 2002; Macatee et al., 2003; Trumpp et al., 1999). A synergistic interaction between Fgf8 and Crkl during formation of the bony palate is manifest by a dramatic increase in the incidence of cleft palate from 5% in $Fgf8^{+/-};Crkl^{+/-}$ or $Crkl^{-/-}$ mutants to 55% in $Fgf8^{+/-};Crkl^{-/-}$ mutants (Figures 1O-1S). Mandibular hypoplasia is apparent in 50% of $Fgf8^{+/-};Crkl^{+/-}$, 60% of $Crkl^{-/-}$, and 85% of $Fgf8^{+/-};Crkl^{-/-}$ mutants (Figure 1U).

Loss of Crkl Decreases Survival of Neural Crest and the Contribution of Neural Crest to the Outflow Tract and Pharyngeal Arches

Neural crest cells (NC) migrate from the dorsal neural tube and make crucial contributions of mesenchyme to the pharyngeal arches, OFT septum, and pharyngeal glands (Jiang et al., 2000). The OFT myocardium is composed of cells derived from the Fgf8-dependent anterior heart field in splanchnic mesoderm (SM) (Kelly and Buckingham, 2002; E. Park and A.M.M., submitted). Abnormal apoptosis of NC and SM in Fgf8 hypomorphs and domain-specific conditional mutants is associated with craniofacial, vascular, and OFT defects (Abu-Issa et al., 2002; Frank et al., 2002; Macatee et al., 2003; E. Park and A.M.M., submitted). We found a marked excess of apoptotic cells in the pharynx of $Crkl^{-/-}$, $Fgf8^{+/-};Crkl^{+/-}$, and $Fgf8^{+/-};Crkl^{-/-}$ mutants, including cells streaming into the pharynx from the neural tube (Figures 2A-2E). Since Crkl is expressed in NC adjacent to Fgf8-expressing domains, we immunohistochemically labeled NC with the marker AP-2a and assayed for apoptosis. This revealed multiple regions of apoptotic NC en route to the pharyngeal arches in $Crkl^{-/-}$, $Fgf8^{+/-};Crkl^{+/-}$, and $Fgf8^{+/-};Crkl^{-/-}$ mutants (Figures 2F-2J). Sections revealed that excess apoptosis occurred in the pharyngeal epithelia and SM, in addition to the NC (Figures 2K-2M′). Levels of apoptosis mirror decreases in Fgf8 and/or Crkl gene dosage.

To evaluate NC populations in $Crkl^{-/-}$ embryos, we labeled this cell lineage by using the Rosa26-Cre reporter and the Wnt1Cre transgene (Jiang et al., 2000). All $Crkl^{+/+}$ and $Crkl^{+/-}$ embryos had dense populations of *lacZ*positive cells throughout the PAs and OFT (Figure 2N,

arrows; data not shown), whereas contribution of NC to these structures was obviously decreased in Crkl$^{-/-}$ mutants (Figure 2O, arrows).

These phenotypes demonstrate that Fgf8 and Crkl genetically interact to regulate the development of structures affected in patients with *del22q11* syndrome and suggest that Crkl is required for normal responses to Fgf8 in multiple morphogenetic pathways during embryogenesis. To investigate whether this interaction reflects the function of Crkl downstream of FgfRs (versus functions in parallel molecular pathways that influence development of these structures), we examined the effects of Crkl deficiency on expression of Fgf8 target genes, activation of MAP kinases, and intracellular biochemical signal transduction in vivo.

Crkl Regulates Expression of Fgf8 Target Genes

Fgf8 signaling stimulates transcription of the ETS domain DNA binding proteins Erm and Pea3 (Firnberg and Neubuser, 2002; Raible and Brand, 2001; Roehl and Nusslein-Volhard, 2001). Fgf/FgfR interactions trigger phosphorylation of Erm protein via activated MAPK/ERKs, causing it to bind its transcriptional targets (Janknecht et al., 1996; O'Hagan et al., 1996; Tsang and Dawid, 2004). Whole-mount in situ hybridization revealed decreased Erm and Pea3 expression in the pharyngeal arches of Crkl$^{-/-}$ mutants, consistent with a role for Crkl in mediating Fgf signals (Figures 3A-3J). Decrements in Erm and Pea3 expression in the pharyngeal arches mirrored those in Fgf8 and Crkl gene dosage, and, in Fgf8$^{+/-}$;Crkl$^{-/-}$ mutants, Erm expression was less than that detected in Fgf8 hypomorphs (data not shown). Altered expression of the Fgf8 target gene Barx1 was noted in the hypoplastic caudal arches of Fgf8$^{+/-}$;Crkl$^{-/-}$ mutants (Figures 3K-3O). Decreased Erm and Pea3 expression correlated with levels of phosphorylated Erk1/2 in the pharyngeal arches and limb buds of Crkl$^{-/-}$ and Fgf8;Crkl compound mutant embryos. In Crkl heterozygote controls (Figure 3Q), high levels of phosphorylated Erk are detected in the pharyngeal epithelium and mesenchyme. In compound mutants and Fgf8 hypomorphs (Figures 3R-3T, and data not shown), this pattern of Erk phosphorylation was lost. Thus, expression of known Fgf8 target genes and activation of MAP kinases in Fgf8-responsive tissues depend on Crkl function in vivo.

Crkl Binds Activated Fgf Receptors 1 and 2 and Is Required for Downstream Cellular Responses to Fgf8

We investigated whether Crkl interacts with FgfRs to mediate Fgf8 signaling. In primary cultures of mouse embryonic fibroblasts (MEFs), FgfR1 and FgfR2 are rapidly tyrosine phosphorylated in response to Fgf8b stimulation (Figures 4A and 4B). These activated receptors bind directly to the SH2 domain of Crkl in vitro (Figure 4C). Furthermore, Crkl forms stable complexes with endogenous FgfR1 and FgfR2 proteins in normal Fgf8b-stimulated MEFs in vivo, indicating that formation of these complexes is a physiologic event (Figure 4D). While association of Crkl with these receptors was readily detectable, only a minute amount of Crk was coimmunoprecipitated with the FgfRs compared to the level of Crk in the cell. Thus, Crkl interacts with activated FgfRs far more efficiently than Crk. It is noteworthy that, in contrast to results obtained with overexpressed or chimeric FgfRs in transformed cell lines (Chellaiah et al., 1999; Larsson et al., 1999; Ornitz et al., 1996), in this primary embryonic culture model, Fgf8 activates FgfR1 in addition to FgfR2.

We further interrogated the role of Crkl in mediating functional responses to Fgf8 in MEFs. Wild-type MEFs migrate robustly toward a source of Fgf8b in a modified Boyden chamber assay, whereas MEFs isolated from Crkl$^{-/-}$ embryos do not ($p = 0.0001$, Figure 5A). Chemotaxis to Fgf8 can be rescued by expression of Crkl from a plasmid transfected into the mutant cells prior to assay (Figure 5A, Crkl$^{-/-}$+CRKL). The fact that Crkl$^{-/-}$ MEFs migrate normally toward serum, epidermal growth factor (EGF), or platelet-derived growth factor (PDGF) (Figures 5A

and 5B) demonstrates that the requisite machinery for cell motility is intact, and that migratory defects observed in Crkl$^{-/-}$ cells reside in Crkl-dependent pathways specific to Fgf8 signal transduction.

The cellular response to Fgfs occurs after Fgf ligand binds to the high-affinity cell surface FgfRs, triggering receptor dimerization, autophosphorylation, and subsequent activation of the Ras/Raf/Mek pathway upstream of Erk1/2 MAP kinases (Hadari et al., 2001; Reuss and von Bohlen und Halbach, 2003). We found that Fgf8b induces robust and sustained activation of Erk1/2 MAP kinases in wild-type MEFs (Figure 5C). In contrast, in Crkl$^{-/-}$ MEFs, Fgf8b induces only minor activation of Erk1/2. Furthermore, the effective minimal concentration of Fgf8b required to induce detectable activation of Erk1/2 is approximately 10-fold greater in Crkl$^{-/-}$ cells (20 ng/ml) than in wild-type cells (2.0 ng/ml,Figure 5D).

Since FgfRs are RTKs, we examined the profile of tyrosine-phosphorylated proteins in MEFs after Fgf8b stimulation, with particular attention paid to the docking protein Frs2. In response to Fgf stimulation, Frs2 links FgfR activation to the Ras/MAPK signaling pathway by targeting signaling molecules to the plasma membrane. For example, activated Frs2 recruits the adaptor protein Grb-2/Sos, which sequentially recruits Ras to the FgfR complex (Hadari et al., 1998, 2001;Kouhara et al., 1997;Larsson et al., 1999). While the overall content of protein tyrosine phosphorylation is comparable in Crkl$^{-/-}$ and wild-type MEFs, some species are relatively hypophosphorylated in Crkl$^{-/-}$ cells after Fgf8b stimulation (Figure 5E). One species has a molecular weight of approximately 90 kDa and comigrates with tyrosinephosphorylated species of Frs2 when the same blot is probed with anti-Frs2 antibody (Figure 5F). Immunoprecipitation confirms that Fgf8b-induced tyrosine phosphorylation of Frs2 depends partially on the presence of Crkl (Figure 5G). Furthermore, the level of Frs2 tyrosine phosphorylation can be titrated in Crkl$^{-/-}$ cells by varying the level of Crkl produced from a transgene (Figure 5H). These findings strongly support the role of Crkl in transducing intracellular biochemical responses to Fgf8 during morphogenesis.

Discussion

We have demonstrated that Fgf8 and Crkl genetically interact in expression domains that regulate the formation of organs and structures affected in human patients with *del22q11* syndrome. Furthermore, we have shown that Crkl mediates Fgf8 signaling in vitro and in vivo through an interaction with FgfRs 1 and 2, providing another mechanism for generating dosage-sensitive, context dependent cellular responses to Fgf signaling by downstream intracellular signal modulation (Dailey et al., 2005; Echevarria et al., 2005; Sivak et al., 2005; Tsang and Dawid, 2004). Fgf8 also signals in Crkl-independent pathway(s) because the phenotypes of Fgf8$^{-/-}$ mutants occur earlier and are more profound than Crkl$^{-/-}$ homozygotes (Meyers et al., 1998).

Disruption of either Tbx1 or Crkl, the mouse orthologs of two 22q11 genes, generates features of *del22q11* syndrome in mice, as does Fgf8 deficiency (Abu-Issa et al., 2002; Frank et al., 2002; Guris et al., 2001; Jerome and Papaioannou, 2001; Lindsay et al., 2001; Merscher et al., 2001). It has become clear that TBX1 dysfunction plays an important role in human *del22q11* syndrome (Yagi et al., 2003). However, phenotypic variability in humans and mice with 22q11-like deletions or single gene mutations supports the existence of modifier genes at 22q11 and elsewhere (Frank et al., 2002; Hu et al., 2004; Lindsay, 2001; Lindsay and Baldini, 2001; Schinke and Izumo, 2001; Vitelli et al., 2002a, 2002b; Yagi et al., 2003). The accompanying paper by Guris and colleagues (Guris et al., 2006 [this issue of Developmental Cell]) demonstrates a genetic interaction between Tbx1 and Crkl and confirms that *del22q11* is a contiguous gene syndrome.

Mounting evidence indicates that Fgf8 operates in critical developmental and molecular pathways with both Crkl and Tbx1 during cardiovascular and pharyngeal development (Figure 6). Fgf8 and Tbx1 are both expressed in the pharyngeal epithelia and mesoderm. The relationship between Tbx1 transcriptional activity and Fgf8 expression appears to be cell-type specific: Fgf8 expression is present in the ectoderm, but is absent in the endoderm of Tbx1 null mutants, and a Tbx1-responsive enhancer regulates expression of an Fgf8 transgene in OFT mesoderm (Hu et al., 2004). Fgf8 genetically interacts with Tbx1 to increase penetrance of aortic arch defects in Tbx1 null heterozygotes (Vitelli et al., 2002b), possibly through mutual effects on Gbx2 (Byrd and Meyers, 2005).

Like Crkl, FgfRs 1 and 2 are ubiquitously expressed in pharyngeal tissues, including neural crest, at E8.5-10.5 (Bachler and Neubuser, 2001; Blak et al., 2005; Orr-Urtreger et al., 1991; Peters et al., 1992; Yamaguchi et al., 1992; Guris et al., 2001; A.M.M., unpublished data). The different sensitivity of heart, vasculature, craniofacial, and limb morphogenesis to altered Crkl and Fgf8 dosage suggests that Crkl functions downstream of multiple Fgf/FgfRs in different morphogenetic pathways and that reliance of a particular Fgf/FgfR signaling event on Crkl-mediated signal transduction is context dependent. We have previously shown that the pharyngeal ectoderm is the source of Fgf8 required for PAA4 formation/remodeling (Macatee et al., 2003). Disrupted PAA4 vasculogenesis in Fgf8;Crkl mutants suggests an early role for Crkl in mediating Fgf signals from the ectoderm. Notably, failed vasculogenesis of PAAs3-6 resulting in mid-gestational lethality of the most severely affected Fgf8;Crkl mutants also occurs after ablation of both Fgf8 and Fgf4 from the pharyngeal ectoderm (L. Francis and A.M.M., unpublished data). OFT septation and alignment are independently regulated by Fgf8 emanating from pharyngeal endoderm and anterior heart field mesoderm, respectively (E. Park and A.M.M., submitted). Thus, the presence of alignment and septation defects in $Fgf8^{+/-}$;$Crkl^{-/-}$ mutants indicates that Crkl also plays a role in transduction of Fgf8 from these expression domains. Although Fgf10 and Fgf4 are not independently required in cardiovascular or craniofacial development (Min et al., 1998; Moon et al., 2000; Sekine et al., 1999; Sun et al., 2000; L. Francis and A.M.M., unpublished data), they are also expressed in the developing heart and pharynx; we are investigating their functional redundancy with Fgf8 and their reliance on Crkl during cardiovascular development.

In vitro mitogenic assays suggest that Fgf ligand/receptor preferences exist (Ornitz and Itoh, 2001; Ornitz et al., 1996), but it has been unclear how preferences exhibited by transformed cells in culture apply to the highly plastic, tissue-specific environments present in developing embryos. Our data indicate that Fgf8b activates both FgfR1 and FgfR2, and that these receptors interact with Crkl in response to Fgf8 stimulation. Moreover, Crkl is required for MAPK activation and high-level phosphorylation of FRS2 in response to Fgf8b in murine embryonic fibroblasts. These findings are consistent with accumulating evidence suggesting that FgfR1 and FgfR2 mediate many responses to Fgf8 (Arman et al., 1998; Celli et al., 1998; Deng et al., 1994, 1997; Rossant et al., 1997; Sun et al., 1999; Trokovic et al., 2003; Xu et al., 1998). We recently discovered that FgfR1 is required in the pharyngeal epithelia to support formation of the PAAs (L. Francis and A.M.M., unpublished data).

Crkl functions in multiple signaling pathways, and, thus, $Crkl^{-/-}$ mutant phenotypes likely represent the effects of altered transduction and integration of FGF and VEGF, EGF, PDGF, and BMP/TGFβ signaling, in addition to perturbed focal adhesion assembly and function (Feller, 2001; Feller et al., 1998; Li et al., 2002, 2003; Presta et al., 2005). For example, $TGF\beta_2$ null mice have DORV, VSD, and dysplastic atrioventricular and outflow valves (Sanford et al., 1997), phenotypes also present in $Crkl^{-/-}$ and Fgf8;Crkl mutants. As in gastrulation and neurulation (Pera et al., 2003), it is likely that Smad-dependent and -independent inputs downstream of TGFβ receptors converge on the Ras/Erk/MAPK and PI3K/Akt pathways, which are also downstream of FgfRs (Derynck and Zhang, 2003; Zhang and

Derynck, 1999). Reduced Fgf8 dosage in Fgf8;Crkl compound mutants impinges further upon Fgf-sensitive pathways impaired by Crkl deficiency, thus providing a biochemical basis for the genetic interactions observed in vivo. These results strongly support the hypothesis that disrupted FGF8 signaling contributes to the pathogenesis of congenital cardiovascular disease, and that FGF8 function may modify phenotypes in humans with 22q11 mutations involving TBX1 or CRKL.

Experimental Procedures

Mice

The Crkl null ($Crkl^-$), Fgf8 hypomorphic ($Fgf8^H$), and Fgf8 null ($Fgf8^-$) alleles were described previously (Frank et al., 2002; Guris et al., 2001; Moon and Capecchi, 2000). These alleles were originally targeted in 129Sv-derived ES cells and then backcrossed 3-4 generations into C57BL/6J prior to interstrain crosses.

In Situ Detection of Apoptosis

Primary and secondary antibodies and the methods employed to detect AP2α in neural crest, TUNEL, and Hoechst staining of nuclei in whole-mount and on cryosectioned specimens were previously described (Macatee et al., 2003). In whole-mount specimens, apoptotic cells were detected with anti-cleaved caspase 3 (Cell Signaling Technology, 9664S).

Marking the Neural Crest

Neural crest cells were genetically labeled by using the R26R and Wnt1Cre strains (kind gifts from P. Soriano and A.P. McMahon, respectively). These strains were maintained by continual backcross with C57BL/6J for more than 11 generations. Embryos were stained with Salmon-gal (Biosynth) by standard protocols.

Whole-Mount In Situ Hybridization

Whole-mount in situ RNA hybridization was performed by using a standard protocol (Guris et al., 2001). Experiments were repeated a minimum of three times.

Whole-Mount Detection of MAP Kinase Activation

Phosphorylated Erk1 and Erk2 were detected as described (Corson et al., 2003), but with minor modifications: rabbit polyclonal antiphosphorylated p44/p42 was used (Cell Signaling Technology, 9101S). After dissection in cold PBS, the embryos were fixed overnight at 4°C, washed in 1× PBS and 0.5% NP40, then dehydrated/rehydrated through a methanol series. Embryos were blocked with 1× PBS/5% goat serum/0.1% Triton X-100 and were incubated overnight at 4°C with primary antibody diluted 1:350 in PBST. Washes were followed by repeated blocking and incubation overnight with secondary antibody (Alexa 594 goat anti-rabbit; diluted 1:200 in PBST). Fluorescence of 2 μm optical sections under a10× objective were recorded with an Olympus 1X70 Fluoview confocal microscope.

Cellular and Biochemical Analysis

Preparation of mouse embryonic fibroblasts and assay of cell motility with a modified Boyden chamber were described previously (Li et al., 2003). Western blots and immunoprecipitation were performed by using standard procedures. GST-CRKL SH2 generated in E. coli was isolated by glutathione-Sepharose beads (GE Biotechnology) prior to pull-down assays.

Rabbit anti-CRKL (C-20), anti-CRK-II (C-18), anti-FGFR1 (C-15), anti-FGFR2 (C-17), and anti-FRS2 (H-91) antibodies were purchased from Santa Cruz Biotechnology. In some experiments, mouse monoclonal anti-CRKL (Upstate Biotechnology), anti-CRK (BD

Pharmingen), and anti-FGFR1 (Zymed) were used for compatible combinations of antibody host species for immunoprecipitation, followed by immunoblot analysis, and for confirmation. Mouse monoclonal anti-phosphotyrosine (PY99) antibody was obtained from Santa Cruz Biotechnology. Anti-phospho Erk p44/42 (pTEpY) monoclonal (E10) and anti-p44/42 polyclonal antibodies were obtained from Cell Signaling Technology.

Acknowledgments

We thank Kirk Thomas, Charles Murtaugh, R.K. Ho, E.M. McNally, and E. Svensson for critical reading of the manuscript; A.P. McMahon and P. Soriano for sharing valuable reagents; and A. Sharma and A. Miller for technical assistance. This work was supported in part by grants from the United States Department of Defense (DAMD17-02-1-0639, A.I.); the United States National Institutes of Health, the National Institute for Dental and Craniofacial Research (R01DE015883, A.I.); the National Institute of Child Health and Human Development (R01HD044157, A.M.M.); and a Grantin-Aid from the American Heart Association (A.M.M.). D.L.G is supported by an MD/PhD training grant from the National Institute of Child Health and Human Development (T32HD007009).

References

Abu-Issa R, Smyth G, Smoak I, Yamamura KI, Meyers EN. Fgf8 is required for pharyngeal arch and cardiovascular development in the mouse. Development 2002;129:4613–4625. [PubMed: 12223417]

Arman E, Haffner-Krausz R, Chen Y, Heath JK, Lonai P. Targeted disruption of fibroblast growth factor (FGF) receptor 2 suggests a role for FGF signaling in pregastrulation mammalian development. Proc. Natl. Acad. Sci. USA 1998;95:5082–5087. [PubMed: 9560232]

Bachler M, Neubuser A. Expression of members of the Fgf family and their receptors during midfacial development. Mech. Dev 2001;100:313–316. [PubMed: 11165488]

Bird LM, Scambler P. Cortical dysgenesis in 2 patients with chromosome 22q11 deletion. Clin. Genet 2000;58:64–68. [PubMed: 10945664]

Blak AA, Naserke T, Weisenhorn DM, Prakash N, Partanen J, Wurst W. Expression of Fgf receptors 1, 2, and 3 in the developing mid- and hindbrain of the mouse. Dev. Dyn 2005;233:1023–1030. [PubMed: 15830353]

Bottcher RT, Niehrs C. Fibroblast growth factor signaling during early vertebrate development. Endocr. Rev 2005;26:63–77. [PubMed: 15689573]

Boulet AM, Moon AM, Arenkiel BR, Capecchi MR. The roles of Fgf4 and Fgf8 in limb bud initiation and outgrowth. Dev. Biol 2004;273:361–372. [PubMed: 15328019]

Byrd NA, Meyers EN. Loss of Gbx2 results in neural crest cell patterning and pharyngeal arch artery defects in the mouse embryo. Dev. Biol 2005;284:233–245. [PubMed: 15996652]

Celli G, LaRochelle WJ, Mackem S, Sharp R, Merlino G. Soluble dominant-negative receptor uncovers essential roles for fibroblast growth factors in multi-organ induction and patterning. EMBO J 1998;17:1642–1655. [PubMed: 9501086]

Chellaiah A, Yuan W, Chellaiah M, Ornitz DM. Mapping ligand binding domains in chimeric fibroblast growth factor receptor molecules. Multiple regions determine ligand binding specificity. J. Biol. Chem 1999;274:34785–34794. [PubMed: 10574949]

Corson LB, Yamanaka Y, Lai KM, Rossant J. Spatial and temporal patterns of ERK signaling during mouse embryogenesis. Development 2003;130:4527–4537. [PubMed: 12925581]

Dailey L, Ambrosetti D, Mansukhani A, Basilico C. Mechanisms underlying differential responses to FGF signaling. Cytokine Growth Factor Rev 2005;16:233–247. [PubMed: 15863038]

Deng CX, Wynshaw-Boris A, Shen MM, Daugherty C, Ornitz DM, Leder P. Murine FGFR-1 is required for early post-implantation growth and axial organization. Genes Dev 1994;8:3045–3057. [PubMed: 8001823]

Deng C, Bedford M, Li C, Xu X, Yang X, Dunmore J, Leder P. Fibroblast growth factor receptor-1 (FGFR-1) is essential for normal neural tube and limb development. Dev. Biol 1997;185:42–54. [PubMed: 9169049]

Derynck R, Zhang YE. Smad-dependent and Smad-independent pathways in TGF-β family signalling. Nature 2003;425:577–584. [PubMed: 14534577]

Echevarria D, Belo JA, Martinez S. Modulation of Fgf8 activity during vertebrate brain development. Brain Res. Brain Res. Rev 2005;49:150–157. [PubMed: 16111545]

Emanuel BS, McDonald-McGinn D, Saitta SC, Zackai EH. The 22q11.2 deletion syndrome. Adv. Pediatr 2001;48:39–73. [PubMed: 11480765]

Feller SM. Crk family adaptors-signalling complex formation and biological roles. Oncogene 2001;20:6348–6371. [PubMed: 11607838]

Feller SM, Posern G, Voss J, Kardinal C, Sakkab D, Zheng J, Knudsen BS. Physiological signals and oncogenesis mediated through Crk family adapter proteins. J. Cell. Physiol 1998;177:535–552. [PubMed: 10092207]

Firnberg N, Neubuser A. FGF signaling regulates expression of Tbx2, Erm, Pea3, and Pax3 in the early nasal region. Dev. Biol 2002;247:237–250. [PubMed: 12086464]

Frank DU, Fotheringham LK, Brewer JA, Muglia LJ, Tristani Firouzi M, Capecchi MR, Moon AM. An Fgf8 mouse mutant phenocopies human 22q11 deletion syndrome. Development 2002;129:4591–4603. [PubMed: 12223415]

Guris DL, Fantes J, Tara D, Druker BJ, Imamoto A. Mice lacking the homologue of the human 22q11.2 gene CRKL phenocopy neurocristopathies of DiGeorge syndrome. Nat. Genet 2001;27:293–298. [PubMed: 11242111]

Guris DL, Duester G, Papaioannou VE, Imamoto A. Dose-dependent interaction of Tbx1 and Crkl and locally aberrant RA signaling in a model of *del22q11* syndrome. Dev. Cell 2006;10:81–92. [PubMed: 16399080]this issue

Hadari YR, Kouhara H, Lax I, Schlessinger J. Binding of Shp2 tyrosine phosphatase to FRS2 is essential for fibroblast growth factor-induced PC12 cell differentiation. Mol. Cell. Biol 1998;18:3966–3973. [PubMed: 9632781]

Hadari YR, Gotoh N, Kouhara H, Lax I, Schlessinger J. Critical role for the docking-protein FRS2 a in FGF receptor-mediated signal transduction pathways. Proc. Natl. Acad. Sci. USA 2001;98:8578–8583. [PubMed: 11447289]

Hu T, Yamagishi H, Maeda J, McAnally J, Yamagishi C, Srivastava D. Tbx1 regulates fibroblast growth factors in the anterior heart field through a reinforcing autoregulatory loop involving forkhead transcription factors. Development 2004;131:5491–5502. [PubMed: 15469978]

Janknecht R, Monte D, Baert JL, de Launoit Y. The ETS-related transcription factor ERM is a nuclear target of signaling cascades involving MAPK and PKA. Oncogene 1996;13:1745–1754. [PubMed: 8895521]

Jerome LA, Papaioannou VE. DiGeorge syndrome phenotype in mice mutant for the T-box gene, Tbx1. Nat. Genet 2001;27:286–291. [PubMed: 11242110]

Jiang X, Rowitch DH, Soriano P, McMahon AP, Sucov HM. Fate of the mammalian cardiac neural crest. Development 2000;127:1607–1616. [PubMed: 10725237]

Kelly RG, Buckingham ME. The anterior heart-forming field: voyage to the arterial pole of the heart. Trends Genet 2002;18:210–216. [PubMed: 11932022]

Klint P, Claesson-Welsh L. Signal transduction by fibroblast growth factor receptors. Front. Biosci 1999;4:D165–D177. [PubMed: 9989949]

Kouhara H, Hadari YR, Spivak-Kroizman T, Schilling J, BarSagi D, Lax I, Schlessinger J. A lipid-anchored Grb2-binding protein that links FGF-receptor activation to the Ras/MAPK signaling pathway. Cell 1997;89:693–702. [PubMed: 9182757]

Larsson H, Klint P, Landgren E, Claesson-Welsh L. Fibroblast growth factor receptor-1-mediated endothelial cell proliferation is dependent on the Src homology (SH) 2/SH3 domain-containing adaptor protein Crk. J. Biol. Chem 1999;274:25726–25734. [PubMed: 10464310]

Lewandoski M, Sun X, Martin GR. Fgf8 signalling from the AER is essential for normal limb development. Nat. Genet 2000;26:460–463. [PubMed: 11101846]

Li L, Okura M, Imamoto A. Focal adhesions require catalytic activity of Src family kinases to mediate integrin-matrix adhesion. Mol. Cell. Biol 2002;22:1203–1217. [PubMed: 11809811]

Li L, Guris DL, Okura M, Imamoto A. Translocation of CrkL to focal adhesions mediates integrin-induced migration downstream of Src family kinases. Mol. Cell. Biol 2003;23:2883–2892. [PubMed: 12665586]

Lindsay EA. Chromosomal microdeletions: dissecting *del22q11* syndrome. Nat. Rev. Genet 2001;2:858–868. [PubMed: 11715041]

Lindsay EA, Baldini A. Recovery from arterial growth delay reduces penetrance of cardiovascular defects in mice deleted for the DiGeorge syndrome region. Hum. Mol. Genet 2001;10:997–1002. [PubMed: 11309372]

Lindsay EA, Vitelli F, Su H, Morishima M, Huynh T, Pramparo T, Jurecic V, Ogunrinu G, Sutherland HF, Scambler PJ, et al. Tbx1 haploinsufficieny in the DiGeorge syndrome region causes aortic arch defects in mice. Nature 2001;410:97–101. [PubMed: 11242049]

Macatee TL, Hammond BP, Arenkiel BR, Francis L, Frank DU, Moon AM. Ablation of specific expression domains reveals discrete functions of ectoderm- and endodermderived FGF8 during cardiovascular and pharyngeal development. Development 2003;130:6361–6374. [PubMed: 14623825]

Merscher S, Funke B, Epstein JA, Heyer J, Puech A, Lu MM, Xavier RJ, Demay MB, Russell RG, Factor S, et al. TBX1 is responsible for cardiovascular defects in velo-cardio-facial/DiGeorge syndrome. Cell 2001;104:619–629. [PubMed: 11239417]

Meyers EN, Lewandoski M, Martin GR. An Fgf8 mutant allelic series generated by Cre- and Flp-mediated recombination. Nat. Genet 1998;18:136–141. [PubMed: 9462741]

Min H, Danilenko DM, Scully SA, Bolon B, Ring BD, Tarpley JE, DeRose M, Simonet WS. Fgf-10 is required for both limb and lung development and exhibits striking functional similarity to Drosophila branchless. Genes Dev 1998;12:3156–3161. [PubMed: 9784490]

Moon AM, Capecchi MR. Fgf8 is required for outgrowth and patterning of the limbs. Nat. Genet 2000;26:455–459. [PubMed: 11101845]

Moon AM, Boulet AM, Capecchi MR. Normal limb development in conditional mutants of Fgf4. Development 2000;127:989–996. [PubMed: 10662638]

Motzkin B, Marion R, Goldberg R, Shprintzen R, Saenger P. Variable phenotypes in velocardiofacial syndrome with chromosomal deletion. J. Pediatr 1993;123:406–410. [PubMed: 8355116]

O'Hagan RC, Tozer RG, Symons M, McCormick F, Hassell JA. The activity of the Ets transcription factor PEA3 is regulated by two distinct MAPK cascades. Oncogene 1996;13:1323–1333. [PubMed: 8808707]

Ornitz DM, Itoh N. Fibroblast growth factors. Genome Biol 2001;2REVIEWS3005.3001-3005.3012

Ornitz DM, Xu J, Colvin JS, McEwen DG, MacArthur CA, Coulier F, Gao G, Goldfarb M. Receptor specificity of the fibroblast growth factor family. J. Biol. Chem 1996;271:15292–15297. [PubMed: 8663044]

Orr-Urtreger A, Givol D, Yayon A, Yarden Y, Lonai P. Developmental expression of two murine fibroblast growth factor receptors, flg and bek. Development 1991;113:1419–1434. [PubMed: 1667382]

Pera EM, Ikeda A, Eivers E, De Robertis EM. Integration of IGF, FGF, and anti-BMP signals via Smad1 phosphorylation in neural induction. Genes Dev 2003;17:3023–3028. [PubMed: 14701872]

Peters KG, Werner S, Chen G, Williams LT. Two FGF receptor genes are differentially expressed in epithelial and mesemchymal tissues during limb formation and organogenesis in the mouse. Development 1992;114:233–243. [PubMed: 1315677]

Presta M, Dell'Era P, Mitola S, Moroni E, Ronca R, Rusnati M. Fibroblast growth factor/fibroblast growth factor receptor system in angiogenesis. Cytokine Growth Factor Rev 2005;16:159–178. [PubMed: 15863032]

Raible F, Brand M. Tight transcriptional control of the ETS domain factors Erm and Pea3 by Fgf signaling during early zebrafish development. Mech. Dev 2001;107:105–117. [PubMed: 11520667]

Reuss B, von Bohlen und Halbach O. Fibroblast growth factors and their receptors in the central nervous system. Cell Tissue Res 2003;313:139–157. [PubMed: 12845521]

Roehl H, Nusslein-Volhard C. Zebrafish pea3 and erm are general targets of FGF8 signaling. Curr. Biol 2001;11:503–507. [PubMed: 11413000]

Rossant J, Ciruna B, Partanen J. FGF signaling in mouse gastrulation and anteroposterior patterning. Cold Spring Harb. Symp. Quant. Biol 1997;62:127–133. [PubMed: 9598344]

Sanford LP, Ormsby I, Gittenberger-de Groot AC, Sariola H, Friedman R, Boivin GP, Cardell EL, Doetschman T. TGFβ2 knockout mice have multiple developmental defects that are non-overlapping with other TGFβ knockout phenotypes. Development 1997;124:2659–2670. [PubMed: 9217007]

Scambler PJ. The 22q11 deletion syndromes. Hum. Mol. Genet 2000;9:2421–2426. [PubMed: 11005797]

Schinke M, Izumo S. Deconstructing DiGeorge syndrome. Nat. Genet 2001;27:238–240. [PubMed: 11242098]

Sekine K, Ohuchi H, Fujiwara M, Yamasaki M, Yoshizawa T, Sato T, Yagishita N, Matsui D, Koga Y, Itoh N, Kato S. Fgf10 is essential for limb and lung formation. Nat. Genet 1999;21:138–141. [PubMed: 9916808]

Sivak JM, Petersen LF, Amaya E. FGF signal interpretation is directed by Sprouty and Spred proteins during mesoderm formation. Dev. Cell 2005;8:689–701. [PubMed: 15866160]

Sun X, Meyers EN, Lewandoski M, Martin GR. Targeted disruption of Fgf8 causes failure of cell migration in the gastrulating mouse embryo. Genes Dev 1999;13:1834–1846. [PubMed: 10421635]

Sun X, Lewandoski M, Meyers EN, Liu YH, Maxson RE Jr. Martin GR. Conditional inactivation of Fgf4 reveals complexity of signalling during limb bud development. Nat. Genet 2000;25:83–86. [PubMed: 10802662]

Trokovic N, Trokovic R, Mai P, Partanen J. Fgfr1 regulates patterning of the pharyngeal region. Genes Dev 2003;17:141–153. [PubMed: 12514106]

Trumpp A, Depew MJ, Rubenstein JL, Bishop JM, Martin GR. Cre-mediated gene inactivation demonstrates that FGF8 is required for cell survival and patterning of the first branchial arch. Genes Dev 1999;13:3136–3148. [PubMed: 10601039]

Tsang M, Dawid IB. Promotion and attenuation of FGF signaling through the Ras-MAPK pathway. Sci. STKE 2004;2004:pe17. [PubMed: 15082862]

Vitelli F, Morishima M, Taddei I, Lindsay EA, Baldini A. Tbx1 mutation causes multiple cardiovascular defects and disrupts neural crest and cranial nerve migratory pathways. Hum. Mol. Genet 2002a; 11:915–922. [PubMed: 11971873]

Vitelli F, Taddei I, Morishima M, Meyers EN, Lindsay EA, Baldini A. A genetic link between Tbx1 and fibroblast growth factor signaling. Development 2002b;129:4605–4611. [PubMed: 12223416]

Xu X, Weinstein M, Li C, Naski M, Cohen RI, Ornitz DM, Leder P, Deng C. Fibroblast growth factor receptor 2 (FGFR2)-mediated reciprocal regulation loop between FGF8 and FGF10 is essential for limb induction. Development 1998;125:753–765. [PubMed: 9435295]

Yagi H, Furutani Y, Hamada H, Sasaki T, Asakawa S, Minoshima S, Ichida F, Joo K, Kimura M, Imamura S, et al. Role of TBX1 in human *del22q11*.2 syndrome. Lancet 2003;362:1366–1373. [PubMed: 14585638]

Yamagishi H, Srivastava D. Unraveling the genetic and developmental mysteries of 22q11 deletion syndrome. Trends Mol. Med 2003;9:383–389. [PubMed: 13129704]

Yamaguchi TP, Conlon RA, Rossant J. Expression of the fibroblast growth factor receptor FGFR-1/flg during gastrulation and segmentation in the mouse embryo. Dev. Biol 1992;152:75–88. [PubMed: 1321062]

Zhang Y, Derynck R. Regulation of Smad signalling by protein associations and signalling crosstalk. Trends Cell Biol 1999;9:274–279. [PubMed: 10370243]

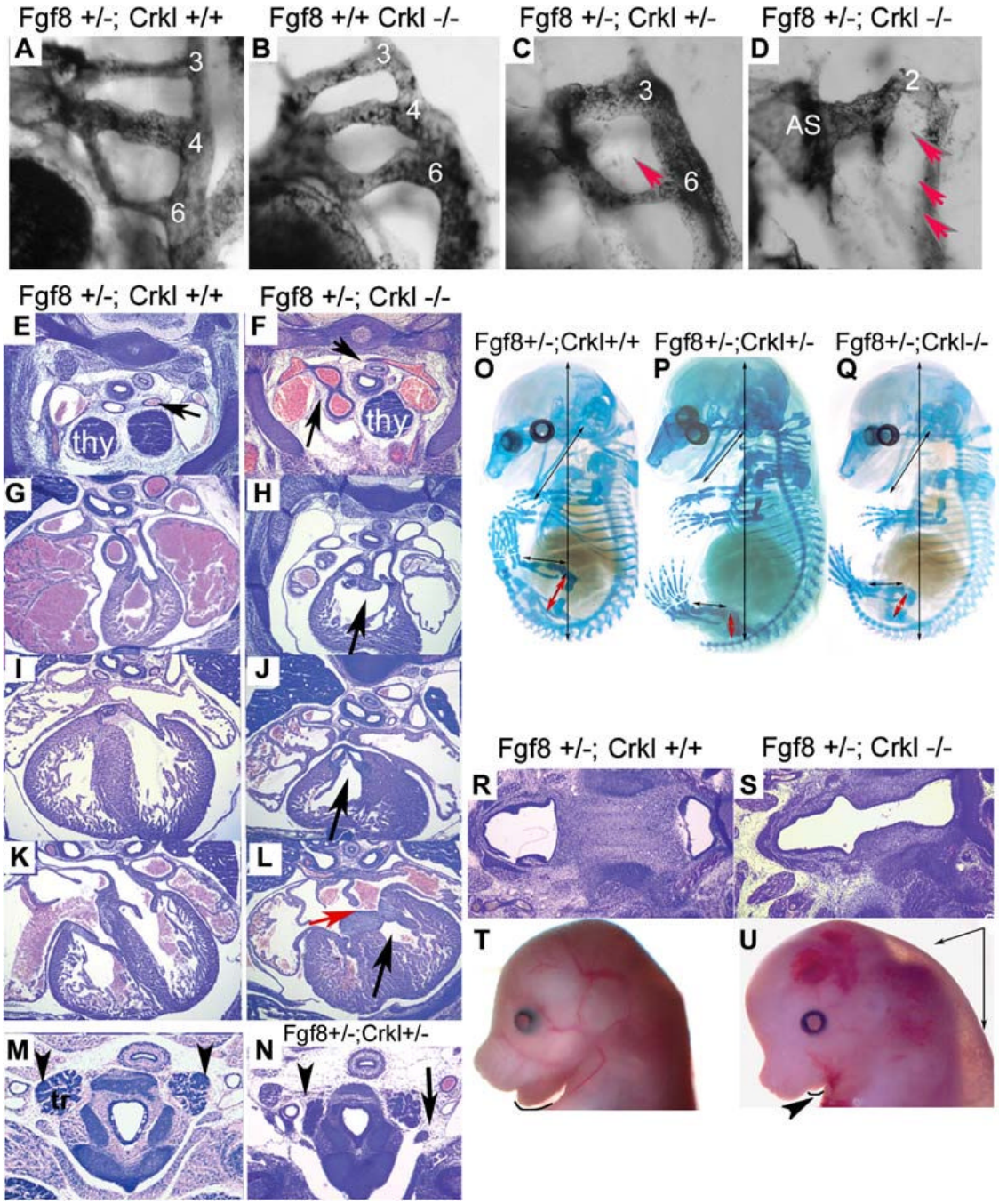

Figure 1.

Crkl and *Fgf8* Genetically Interact during Cardiovascular, Pharyngeal, and Skeletal Development

(A-D) Pharyngeal arch artery (PAA) formation assessed by intracardiac ink injections at embryonic day (E) 10.5. Normal PAA formation and patterning in (A) *Fgf8*$^{+/-}$;Crkl$^{+/+}$and (B) *Fgf8*$^{+/+}$;Crkl$^{-/-}$ embryos. PAA4 or PAA3-PAA6 vasculogenesis fails (red arrowheads) in (C) *Fgf8*$^{+/-}$;Crkl$^{+/-}$ and (D) *Fgf8*$^{+/-}$;Crkl$^{-/-}$ mutants associated with a dilated aortic sac (AS, [D]). PAAs are numbered.

(E-M) (E, G, I, K, and M) Transverse sections through the neck and thorax of E15.5 *Fgf8*$^{+/-}$; Crkl$^{+/+}$ control embryos reveal a (E) normal left aortic arch, (G) right ventricular OFT, (I)

continuity of aortic and mitral valves, (I and K) intact atrial and ventricular septae, and (K) atrioventricular valves. Thymus (thy, [E]), thyroid (tr, [E]), and parathyroids (arrowheads, [M]) are normally located and sized. (F, H, J, and L) *Fgf8*$^{+/-}$;Crkl$^{-/-}$ mutants display: ectopic, single-lobed thymi (thy, [F]) or bilateral thymic aplasia; right aortic arch (arrow, [F]) and aberrant subclavian artery (arrowhead, [F]); (H and J) outflow tract defects, including a Double Outlet Right Ventricle with a dysplastic common aortic/pulmonary valve (arrow, [H]) or an aortic valve communicating with the right ventricle (arrow, [J]); endocardial cushion defects, including a primum atrial septal defect (red arrow, [L]) and mitral and tricuspid valve dysplasia (black arrow, [L]).

(N) *Fgf8*$^{+/-}$;Crkl$^{+/-}$ mutant with unilateral parathyroid aplasia (arrowhead) and ectopy (arrow).

(O-Q) Skeleton preparations at E15.5 reveal markedly short femurs (red double arrows) in *Fgf8*;Crkl mutants, even in mutants with longer crown-rump lengths than (P) controls (the black, vertical double arrow is the same length in all specimens).

(R-U) Palate and jaw defects. Sections through the palate reveal complete bony fusion of the palatal shelves (ps) in (R) control versus unfused shelves causing cleft in (S) mutants (arrow). (U) 30% of *Fgf8*$^{+/+}$;Crkl$^{+/-}$, 50% of *Fgf8*$^{+/-}$;Crkl$^{+/-}$, and 70% of *Fgf8*$^{+/-}$; Crkl$^{-/-}$ mutants have short, narrow mandibles (arrowhead). Note the severe edema in the Crkl$^{-/-}$ mutant (arrows, [U]).

fl, forelimbs.

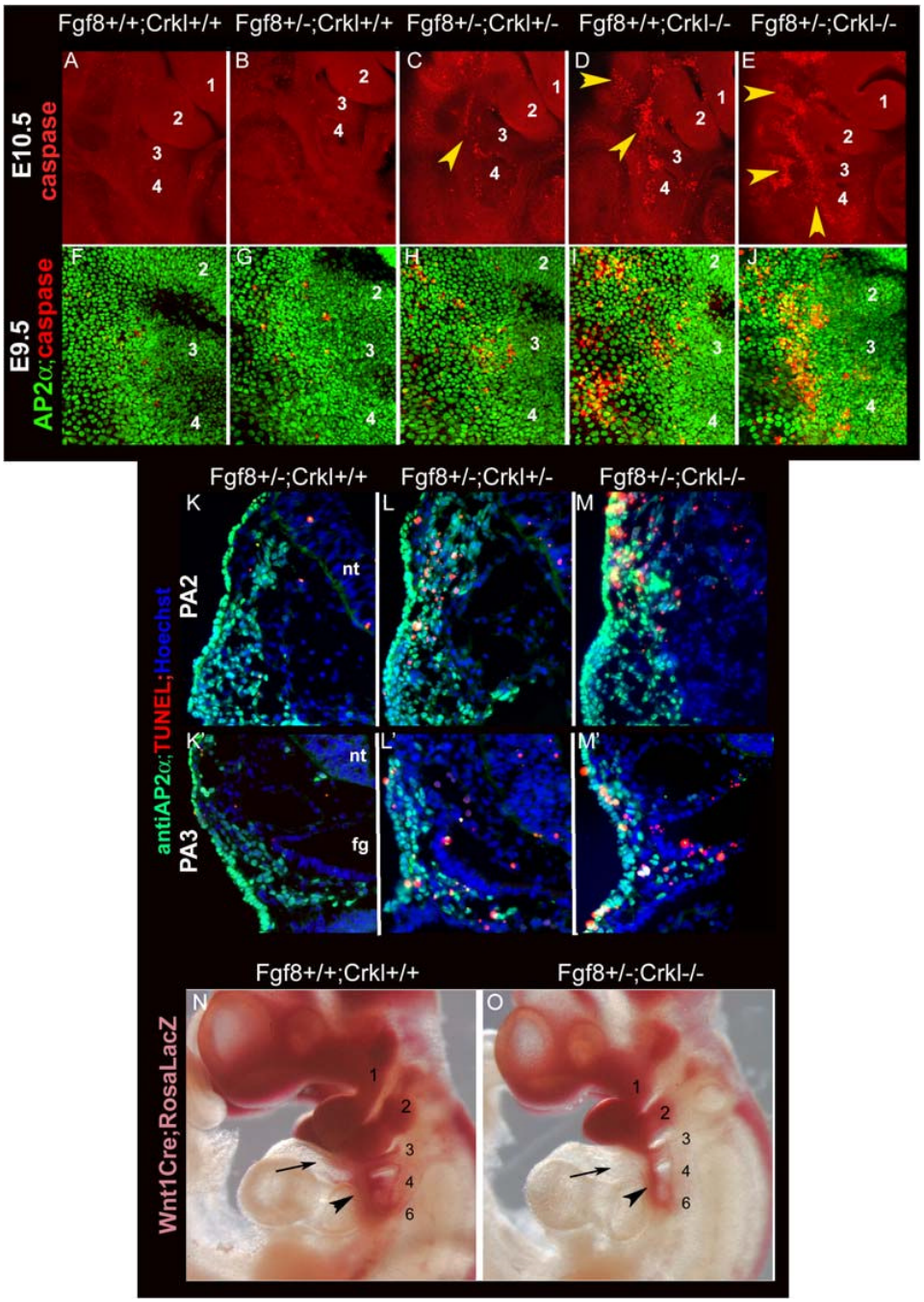

Figure 2.

Decreased Neural Crest Population of the Outflow Tract and Caudal Pharyngeal Arches of Crkl$^{-/-}$ Embryos Is Associated with Abnormal Apoptosis

Genotypes are listed above the columns, and assay type is listed at the left; pharyngeal arches are numbered.

(A-E) Whole-mount E10.5 allelelic series assayed for apoptosis with antiactivated caspase3. Right, lateral views at 803. The yellow arrowheads indicate domains of abnormal apoptosis in *Fgf8*;Crkl and Crkl$^{-/-}$ mutants, including streams of neural crest (NC) originating in the hindbrain.

(F-J) Whole-mount preparations of E9.5 allelic series assayed for the NC/ectoderm marker AP2α (green) and antiactivated caspase3 (red); right, lateral views at 3203. Yellow colabeled cells are apoptotic NC and ectoderm.
(K-M) E9.5 transverse cryosections through the second pharyngeal arch assayed for AP2α (green) and apoptosis (TUNEL, red); nuclei are stained blue with Hoechst. Note the multiple cell types undergoing aberrant apoptosis including: NC (double-labeled, yellow), pharyngeal ectoderm, endoderm, and splanchnic mesoderm. nt, neural tube.
(K′-M′) As above, sections through the third pharyngeal arch. fg, foregut.
(N and O) Wnt1Cre and Rosa26-Cre reporter (R26R) strains were used to label NC derivatives in E10.5 $Crkl^{-/-}$ and wild-type embryos. Cells stained red outside the neural tube are NC derivatives. The outflow tract of the (O) mutant is minimally stained compared to (N) wild-type. NC cells extend from dorsal to ventral in the PAs of wild-type embryos, but these extensions are not continuous or as extensive in the caudal PAs of the $Crkl^{-/-}$ mutants (arrowheads). Arrows indicate the OFT/aortic sac.

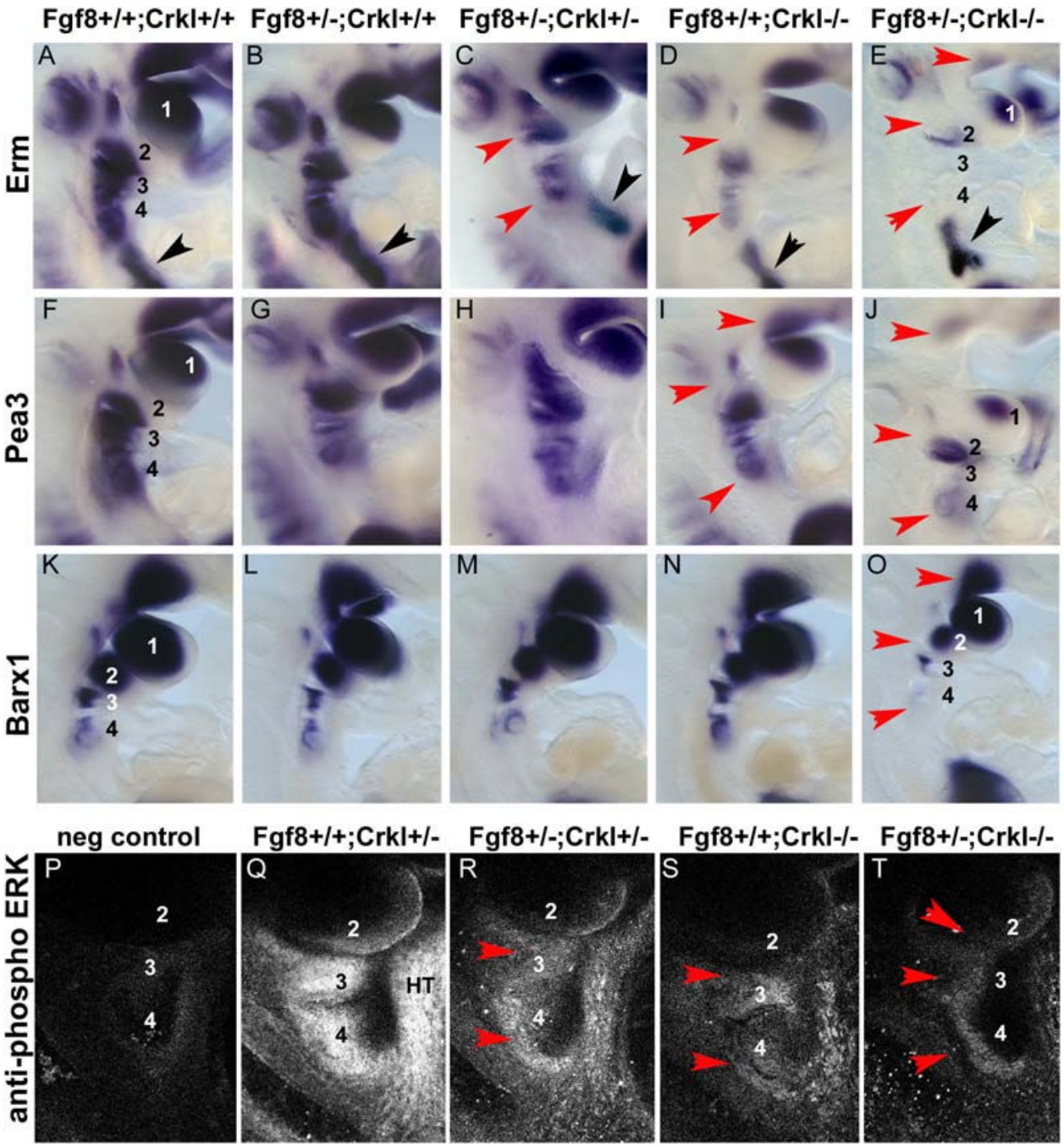

Figure 3.

Crkl Dosage Regulates Expression of Fgf8 Target Genes and Alters MAPK Activation In Vivo

Genotypes are listed above the columns; all views are tight. Lateral and pharyngeal arches are numbered.

(A-E) Right, lateral views of pharyngeal arches of E10.5 embryos after whole-mount in situ hybridization with an Erm antisense riboprobe. Note the decreasing levels of expression in the pharyngeal arches (red arrowheads) of (C) *Fgf8*$^{+/-}$;Crkl$^{+/-}$,(D) Crkl$^{-/-}$, and (E) *Fgf8*$^{+/-}$;Crkl$^{-/-}$ mutants relative to (A and B) controls. Expression in the lung bud (black arrowheads) is intact.

(F-J) As above, after whole-mount in situ hybridization with a Pea3 antisense riboprobe.

(K-O) As above, after whole-mount in situ hybridization with a Barx1 antisense riboprobe.

(P-T) Anti-phospho-Erk1/2 staining of E10.5 embryos. Optical confocal sections were obtained at 2 μm intervals; representative, anatomically matched section images are shown through the casudal PAs. The levels of these activated MAP kinases are decreased (red arrowheads) in the pharyngeal epithelia and mesenchyme in response to decreased Crkl and/or *Fgf8* gene dosage. HT, heart.

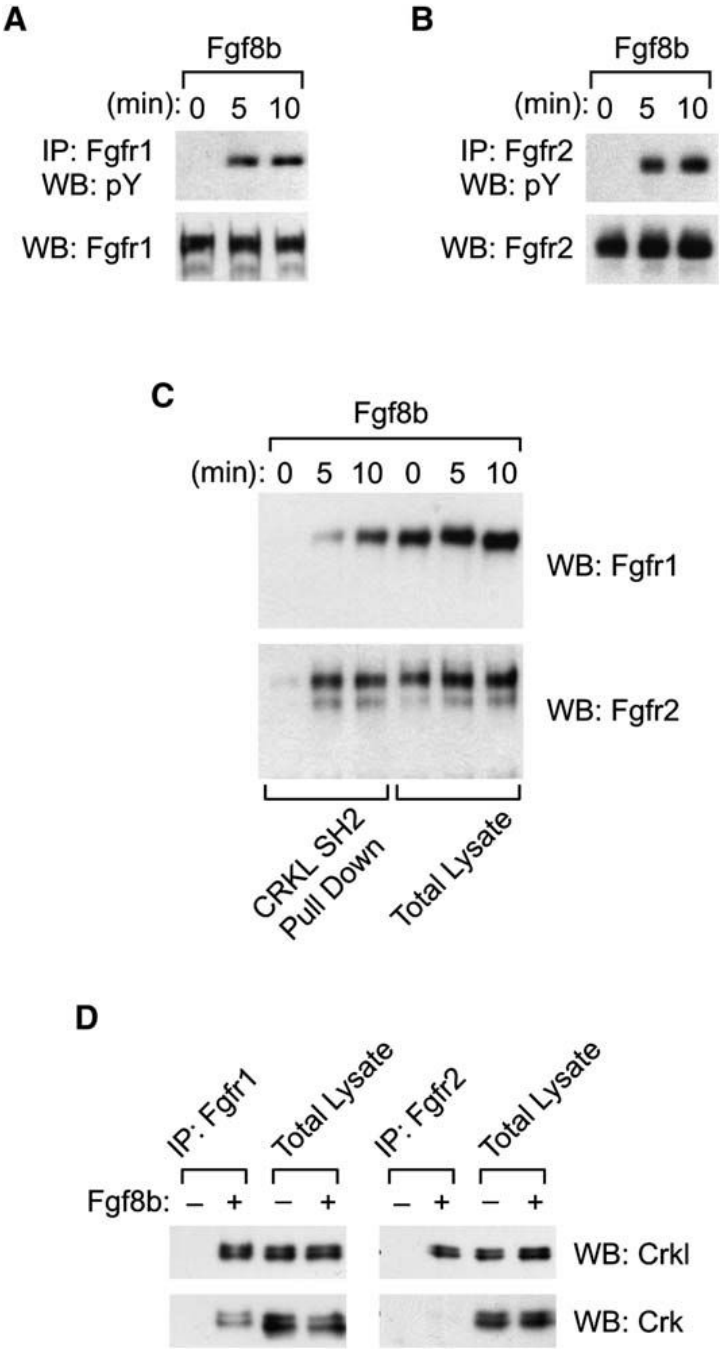

Figure 4.

Fgf Receptors 1 and 2 Are Activated, and Interact with Crkl, in Response to Fgf8

(A and B) Fgf8 stimulates tyrosine phosphorylation of FgfR1 and FgfR2. Anti-receptor antibodies were used to immunoprecipitate Fgf8b-treated MEF lysates (IP), and the products were separated by electrophoresis. Immunoblotting (WB) with anti-phosphotyrosine antibody (pY) reveals that phosphorylation of both receptors occurs in response to 10 ng/ml Fgf8b.

(C) Activated FgfRs interact with Crkl via its SH2 domain. MEFs were treated with 10 ng/ml Fgf8b, and proteins from lysates that bind to the SH2 domain of Crkl were pulled down with GST-Crkl SH2 coupled to glutathione-Sepharose beads. Total MEF lysates (total lysate) or

proteins pulled down (CRKL SH2 pull-down) were blotted and probed with anti-FgfR1 or anti-FgfR2 antibodies (WB).
(D) Endogenous FgfRs associate with Crkl, preferentially with Crk. Proteins that interact with endogenous FgfR1 or FgfR2 were precipitated from control, and Fgf8b-treated MEF lysates were precipitated with anti-FgfR antibody-coupled protein A agarose beads (IP). Immunoprecipitates were separated by electrophoresis and probed with anti-Crkl or -Crk antibody (WB). The relative level of Crkl or Crk in 10 mg total lysate was determined in parallel compared to that associated with FgfR (total lysate).

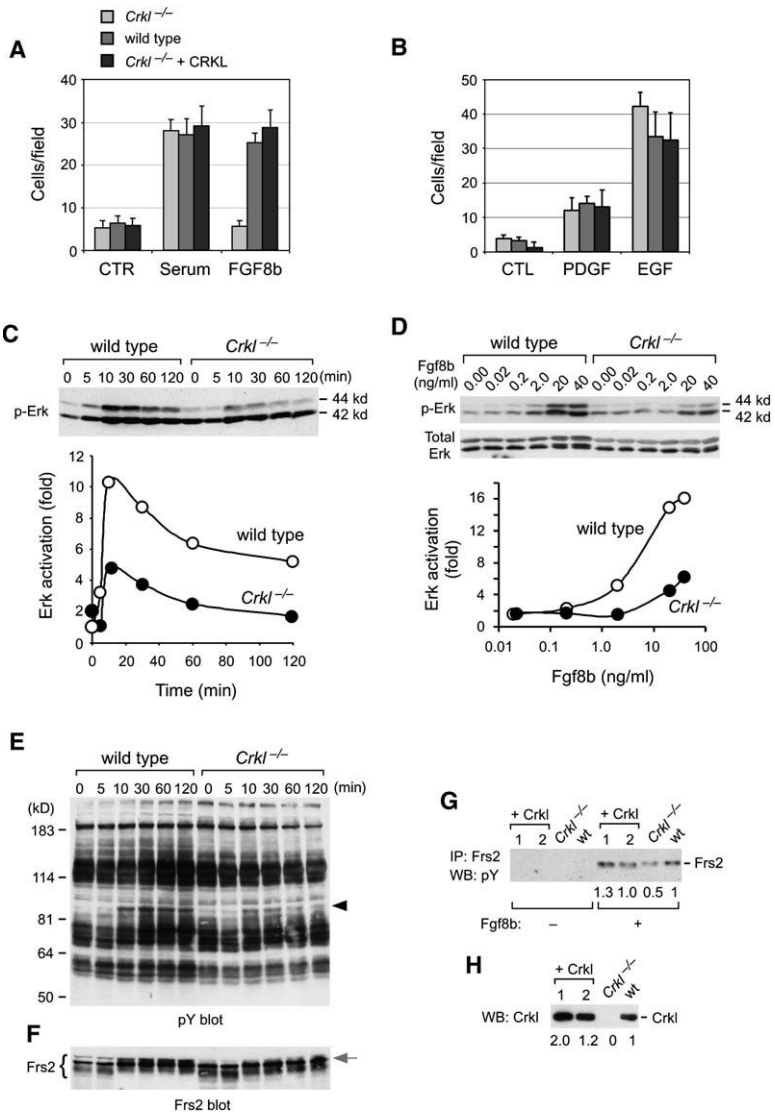

Figure 5.

Crkl Is Required for Fgf8-Induced Chemotaxis and Activation of Downstream Biochemical Signaling Mediators WB, western blot; IP, immunoprecipitation. (A and B) Modified Boyden chamber assay of Crkl$^{-/-}$ MEFs migrating toward Fgf8b ([A], 10 ng/ml), fetal bovine serum ([A], 5%), PDGF ([B], 50 ng/ml), or EGF ([B], 20 ng/ml) compared to wild-type MEFs, or Crkl$^{-/-}$ MEFs expressing CRKL as a transgene at a level comparable to wild-type cells. Control groups (CTR) had buffer with no growth factor or serum in the chambers. Error bars indicate standard deviation of sample data (n = 4).

(C and D) Maximal MAPK activation in response to Fgf8b is Crkl dependent. (C) Cell lysates were prepared after incubation with 25 ng/ml Fgf8b and phosphorylated Erk1 and Erk2 were detected by Western blot. Average phospho-Erk levels (n = 2) are graphically represented as fold activation relative to that at 0 min in wild-type cells. Reblotting with anti-Erk antibody indicated equal levels of total Erk1/2 proteins (not shown). (D) MEFs exposed to varying concentrations of Fgf8b were tested for activation of Erk1 (p44) and Erk2 (p42). Cell lysates were prepared after 10 min of incubation with Fgf8b at the concentrations listed. The average phospho-Erk levels (Erk1 + Erk2) in two experiments are graphically represented below as

fold activation relative to unstimulated levels. The levels of phospho-Erk were normalized relative to the corresponding total Erk levels (Erk1 + Erk2).

(E-H) (E) Crkl regulates the level of Fgf receptor substrate 2 (Frs2) phosphorylation in response to Fgf8b. Anti-phosphotyrosine (pY) blot of total cell lysates prepared at the time indicated after incubation with 25 ng/ml Fgf8b. Black arrowheads indicate a 90 kDa protein phosphorylated in response to Fgf8b; note the decreased intensity of this band in $Crkl^{-/-}$ MEFs at all time points. (F) Anti-Frs2 antibody reprobe of blot shown in (E); the black line denotes Fgf8-stimulated phosphorylation of Frs2 (corresponds to the black arrowhead on the pY blot), This species of Frs2 is relatively hypophosphorylated in $Crkl^{-/-}$ MEFs. (G) Anti-phosphotyrosine blot of Frs2 immunoprecipitated from Fgf8b-stimulated MEFs. “+Crkl” samples are two different $Crkl^{-/-}$ cell lines infected with Crkl-producing retrovirus (see [H]); Fgf8b-stimulated phosphorylation of Frs2 occurs at 1.3× and 1.0× wild-type levels in these cell lines, while that in $Crkl^{-/-}$ MEFs is only 0.5×. (H) Quantitation of Crkl levels: the +Crkl cell line 1 produces Crkl at 2× compared to wild-type levels, and the +Crkl cell line 2 produces Crkl protein at 1.2× compared to wild-type levels.

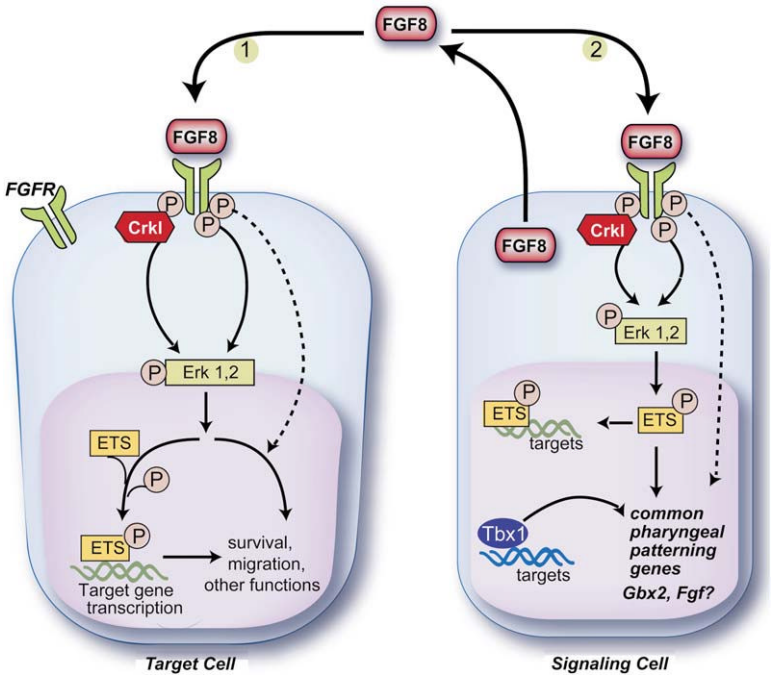

Figure 6.

A Model for Interaction between Crkl-Modulated Fgf Signaling and Tbx1 Function in the Developing Pharyngeal Arches Secreted Fgf8 signals to target cells via paracrine (1) or autocrine (2) pathways. Ligandstimulated FgfR activation triggers receptor autophosphorylation and interaction with signaling mediators, including Crkl. Erk-dependent and -independent pathways affect gene expression, cell survival, and other functions. Phosphorylated MAPK/ERKs downstream of Crkl activate existing ETS proteins (e.g., Erm) and also stimulate their transcription. Tbx1 is expressed in FgfR-expressing pharyngeal mesoderm, ectoderm, and endoderm; in these cells, Tbx1 and Fgf signaling may regulate expression of common transcriptional targets such as Gbx2. Furthermore, both Fgf8 and Tbx1 have been shown to have non-cell autonomous effects on neural crest survival and function.

Table 1

Decrements in Fgf8 and Crkl Cause Cardiovascular and Glandular Defects

	Vascular Defects		Heart/Outflow Tract Defects					
Phenotype, E15.5; Genotype, Fgf8;Crkl	**SCA; HCSCA**	**RAA, IAAB**	**VSD**	**DORV; TA**	**Semilunar Valve Defect**	**ECC**	**Thymic Ectopy, Hypoplasia**	**Parathyroid Ectopy, Hypoplasia, or Aplasia**
+/+; +/+; n = 17	0	0	0	0	0	0	0	1 (6)
+/+; +/-; n = 14	0	0	0	0	0	0	0	1 (7)
+/-; +/+; n = 21	0	0	0	0	0	0	0	2 (10)
+/-; +/-; n = 30	4; 0[a](13;0)	0	2[a](7)	0	0	2[a](7)	9[b](30)	18[b](60)
+/+; -/-; n = 16	0; 4[b](0;25)	2 (13)	16[b](100)	7[b]; 0 (44)	4[b](25)	7[b](44)	5 (31)	10, (63)
+/-; -/-; n = 27	15[b]; 2 (55;7)	11[b](40) 27 (100)	27 (100)	16; 1 (60;4)	13 (48)	19[b](70)	18[b(67c)]	22 (81[c])

Percents are in parentheses; totals may exceed 100% due to multiple phenotypes in a single specimen. SCA, retro-esophageal right or isolated left subclavian artery; HCSCA, high cervical right subclavian artery; VSD, ventricular septal defect; DORV, double outlet right ventricle; TA, persistent Truncus Arteriosus; RAA, circumflex right aortic arch; IAAB, interrupted aortic arch type B; ECC, endocardial cushion defect, mitral, and/or tricuspid valve dysplasia.

[a] Incidence of combined cardiovascular defects was statistically different than in the control.

[b] Statistical significance for the p value was less than 0.05 by using Fisher's exact test comparing with cell in row above.

[c] Glandular defects in Crkl2/2and Fgf8+/2;Crkl2/+mutants were usually unilateral hypoplasia, while, in Fgf8+/2;Crkl2/2mutants, bilateral defects and aplastic glands were more common.